Electronic structure of $SrVO_3$ within $GW + DMFT$

R. Sakuma,[1] Ph. Werner,[2] and F. Aryasetiawan[1]
[1]*Department of Physics, Division of Mathematical Physics, Lund University, Sölvegatan 14A, 223 62 Lund, Sweden*
[2]*Department of Physics, University of Fribourg, 1700 Fribourg, Switzerland*
(Received 24 July 2013; revised manuscript received 16 October 2013; published 10 December 2013)

We present a detailed calculation of the electronic structure of $SrVO_3$ based on the $GW + DMFT$ method. We show that a proper inclusion of the frequency-dependent Hubbard U *and* the nonlocal self-energy via the GW approximation, as well as a careful treatment of the Fermi level, are crucial for obtaining an accurate and coherent picture of the quasiparticle band structure and satellite features of $SrVO_3$. The $GW + DMFT$ results for $SrVO_3$ are not attainable within the GW approximation or the $LDA + DMFT$ scheme. We also compare the results of $GW + DMFT$ to DMFT calculations based on the GW quasiparticle bands.

DOI: 10.1103/PhysRevB.88.235110 PACS number(s): 71.20.−b, 71.27.+a

I. INTRODUCTION

Describing the electronic structure of correlated materials fully from first principles is one of the great challenges in modern condensed matter physics. The dynamical mean-field theory (DMFT)[1–3] in combination with the local density approximation (LDA), known as the $LDA + DMFT$ scheme,[4–7] has in many cases provided a realistic description of the electronic structure and spectral functions of correlated materials. This method, however, suffers from a number of conceptual problems. One of them is the double-counting problem that arises from the difficulty in subtracting the contribution of the LDA exchange-correlation potential in the correlated subspace. Another shortcoming is the DMFT assumption that the self-energy is local. A recent study based on the GW approximation (GWA)[8–11] indicates that even in correlated materials, such as $SrVO_3$, the nonlocal self-energy has a non-negligible influence on the electronic structure. In particular, it was found that the nonlocal self-energy widens the bandwidth significantly.[12]

A decade ago, a different first-principle scheme was proposed, which combines the GWA and the DMFT. This $GW + DMFT$ scheme[13] has the potential of curing the main shortcomings of both the GWA and the DMFT. It goes beyond the GWA by including onsite vertex corrections via the DMFT. Alternatively, from the DMFT point of view, the scheme incorporates a nonlocal self-energy via the GWA. $GW + DMFT$ calculations are fully first principles and self-contained in the sense that the Hubbard U needed in DMFT can in principle be determined self-consistently. Moreover, they do not suffer from the double-counting problem.

In the present work, we apply the $GW + DMFT$ scheme to the much studied cubic perovskite $SrVO_3$, generally considered to be a prototype of correlated metals, as is evident from the large number of both experimental[14–22] and theoretical works.[23–31] Experimentally, a substantial t_{2g} band narrowing by a factor of two compared with the LDA bandwidth is observed.[20] In addition, there are satellite features a few eV below and above the Fermi level, interpreted as the lower and upper Hubbard bands.[14–16,20] Intriguing kinks at low energies are also observed in photoemission experiments.[22]

A consistent description of the electronic structure of $SrVO_3$ that reproduces all these features provides a stringent test for first-principles schemes, since both the satellite features *and* the quasiparticle band structure must be correctly described. $LDA + DMFT$ calculations with a static U yield a band narrowing by a factor of two if a large value of $U = 5.5$ eV is used,[27] but this results in a too large separation of the Hubbard bands.[26] Recent GW calculations on the other hand yield neither the correct band narrowing nor a correct description of the Hubbard bands[12] even when the so-called quasiparticle self-consistent GW scheme is employed.[32] This indicates that vertex corrections beyond the GWA must be included, as supported also by a recent study on the α-γ transition in cerium.[33]

Applications of the $GW + DMFT$ method are rather scarce, and the existing works[34,35] have focused mainly on the spectral functions and Hubbard bands, which are essentially determined by U, whereas little attention has been paid to the quasiparticle band structure, which depends on precise details of the self-energy. Moreover, Ref. 35 used a static U rather than a frequency-dependent U. Applications to a Hubbard model[36–38] and to surface systems within a tight-binding description[39] have also been carried out. Here, by focusing on the self-energy and the quasiparticle band structure, we will demonstrate that both the frequency-dependent U *and* the nonlocal self-energy, as well as a careful treatment of the chemical potential, are essential for obtaining an accurate and coherent description of the electronic structure of $SrVO_3$ entirely from first principles. The picture that emerges is distinct from either the pure GW or the DMFT pictures and thus reveals the importance of the nonlocal self-energy, missing in the DMFT treatment, and the onsite vertex corrections, which are missing in the GWA.

II. THEORY: THE $GW + DMFT$ METHOD

The $GW + DMFT$ method was proposed in Ref. 13 and may be implemented at various levels of self-consistency. Here we describe and test the scheme in its simplest form, where the self-energy is obtained by combining the usual perturbative (non-self-consistent) GW self-energy and the local DMFT self-energy for an impurity model with dynamically screened interaction, and by subtracting a properly defined double-counting term. Progress in solving the DMFT impurity problem with dynamic U by means of continuous-time quantum Monte Carlo (CT-QMC) methods[40–44] has made a proper implementation of this $GW + DMFT$ scheme possible.

Our calculations are based on the strong-coupling CT-QMC technique explained in Refs. 43 and 45.

In the $GW+$DMFT scheme the total self-energy is given by the sum of the GW self-energy and the DMFT impurity self-energy with a double-counting correction:

$$\hat{\Sigma}(\omega) = \sum_{\mathbf{k}nn'} |\psi_{\mathbf{k}n}\rangle\, \Sigma^{GW}_{nn'}(\mathbf{k},\omega)\, \langle\psi_{\mathbf{k}n'}| + \sum_{mm'} |\varphi_m\rangle \left[\Sigma^{\rm imp}_{mm'}(\omega) - \Sigma^{\rm DC}_{mm'}(\omega)\right] \langle\varphi_{m'}|\,, \quad (1)$$

where the $\{\psi_{\mathbf{k}n}\}$ are the LDA Bloch states and the $\{\varphi_m\}$ are the Wannier orbitals constructed from the vanadium t_{2g} bands. The GW self-energy and the impurity self-energy are calculated separately; the latter is obtained from the LDA + DMFT scheme with dynamic U.[46] The double-counting correction $\Sigma^{\rm DC}$ is the contribution of Σ^{GW} to the onsite self-energy which is already contained in the impurity self-energy $\Sigma^{\rm imp}$ calculated within the DMFT with dynamic U. The explicit formula for the double-counting correction is

$$\Sigma^{\rm DC}_{mm'}(\omega) = i \sum_{m_1 m_2 \subset t_{2g}} \int \frac{d\omega'}{2\pi} G^{\rm loc}_{m_1 m_2}(\omega+\omega') W^{\rm loc}_{mm_1,m_2m'}(\omega'), \quad (2)$$

where $G^{\rm loc}(\omega) = \sum_{\mathbf{k}} S^{\dagger}(\mathbf{k}) G(\mathbf{k},\omega) S(\mathbf{k})$ is the onsite projection of the lattice Green function of the t_{2g} subspace, with $S(\mathbf{k})$ the transformation matrix that yields the maximally localized Wannier orbitals according to the prescription of Marzari and Vanderbilt.[47,48] We employ a recently proposed symmetry-constrained routine[49] to construct symmetry-adapted Wannier functions using a customized version of the Wannier90 library.[50] In Eq. (2), $W^{\rm loc}$ is *not* the local part of the usual screened Coulomb interaction, but it is the screened interaction corresponding to the impurity problem in DMFT with the frequency-dependent interaction,

$$W^{\rm loc}(\omega) = [1 - U^{\rm loc}(\omega) P^{\rm loc}(\omega)]^{-1} U^{\rm loc}(\omega). \quad (3)$$

Here, $U^{\rm loc}(\omega)$ is the onsite Hubbard U of the impurity problem calculated using the constrained random-phase approximation (cRPA),[51] and $P^{\rm loc} = -iG^{\rm loc}G^{\rm loc}$ is the local polarization for each spin channel. The matrix elements of $W^{\rm loc}$ are defined as

$$W^{\rm loc}_{mm_1,m_2m'}(\omega) = \int d^3r d^3r' \varphi^*_m(\mathbf{r}) \varphi_{m_1}(\mathbf{r}) W^{\rm loc}(\mathbf{r},\mathbf{r}';\omega) \times \varphi^*_{m_2}(\mathbf{r}') \varphi_{m'}(\mathbf{r}'). \quad (4)$$

The quasiparticle band structure is obtained from the solution of

$$E_{\mathbf{k}n} - \varepsilon_{\mathbf{k}n} - {\rm Re}\Sigma_{nn}(\mathbf{k}, E_{\mathbf{k}n}) = 0, \quad (5)$$

where $\Sigma_{nn}(\mathbf{k},\omega) = \langle\psi_{\mathbf{k}n}|\hat{\Sigma}(\omega)|\psi_{\mathbf{k}n}\rangle$ and $\hat{\Sigma}(\omega)$ is given in Eq. (1). In calculating the quasiparticle energies, the shift of the Fermi level is taken into account according to Hedin's prescription.[52] In this work, the LDA and GW calculations have been performed using the full-potential linearized augmented plane-wave codes FLEUR and SPEX.[53,54]

III. RESULTS AND DISCUSSIONS

A. Quasiparticle band structure

Angle-resolved photoemission (ARPES) measurements reveal a clear t_{2g} quasiparticle band dispersion and a broad almost structureless incoherent feature centered at -1.5 eV below the Fermi level.[20] A mass enhancement by a factor of 2 near the Fermi level is observed[20] consistent with the electronic specific-heat coefficient γ within the Fermi-liquid picture.[15]

In Fig. 1 we present the quasiparticle band structure obtained from several approaches. The bandwidth within LDA, GW, LDA + DMFT, and GW + DMFT are, respectively, 2.6, 2.1, 0.9, and 1.2 eV. From the measured mass enhancement of 2 with respect to the LDA, one may infer that the experimental bandwidth should be approximately 1.3 eV. Upon inclusion of the self-energy correction within the GWA, the LDA band is narrowed to 2.1 eV, which is still much too wide in comparison with the experimental value. The LDA + DMFT quasiparticle bandwidth is 0.9 eV, which is too narrow compared to experiment. As pointed out in an earlier work,[12] the nonlocal self-energy tends to widen the band. Indeed, when the nonlocal self-energy is taken into account within the $GW+$DMFT scheme, the DMFT bandwidth increases to 1.2 eV, in good agreement with the experimental result. Starting from the GW band, the result may also be interpreted as a band narrowing due to onsite vertex corrections.[55] Since little experimental data is available for the unoccupied part of the band, it may be more reliable to compare the occupied part of the calculated band with experiment. From ARPES data[20] the bottom of the occupied band is within -0.7 eV, which is to be compared with -0.6 eV in $GW+$DMFT whereas the corresponding

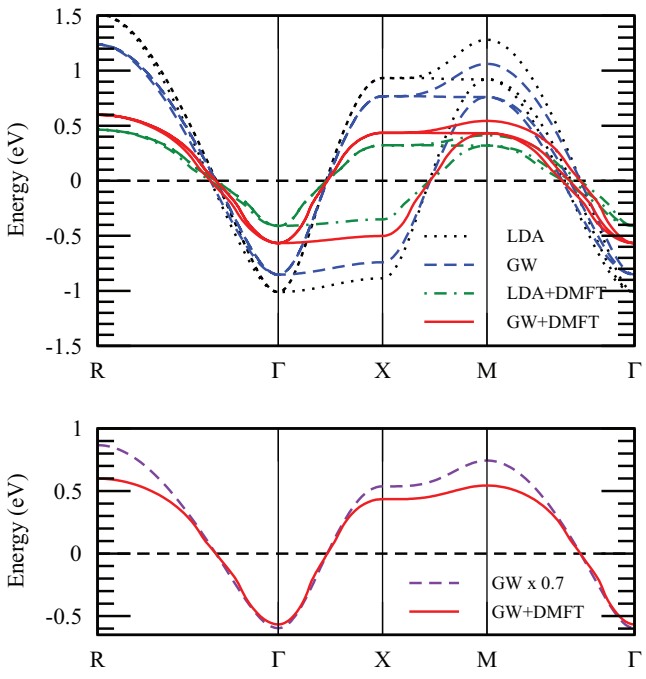

FIG. 1. (Color online) Upper panel: the quasiparticle band structure of $SrVO_3$ within LDA, GW, LDA + DMFT, and $GW+$DMFT. Lower panel: To emphasize the kink structure near Γ, the $GW+$DMFT band is plotted against a renormalized GW band.

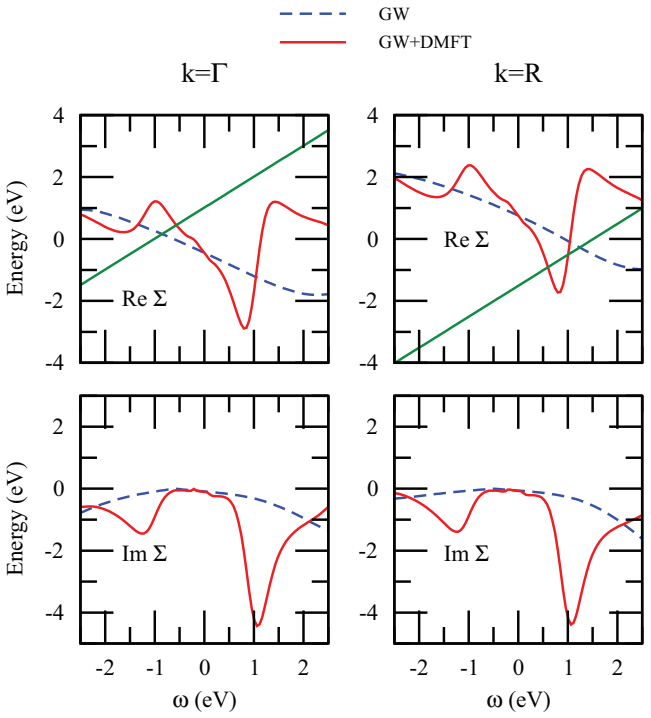

FIG. 2. (Color online) GW and GW + DMFT self-energies at the Γ and R points. The straight line is $\omega - \varepsilon_{\mathbf{k}n}$ where $\varepsilon_{\mathbf{k}n}$ is the LDA energy.

values for LDA, GW, and LDA + DMFT are, respectively, −1.0, −0.9, and −0.4 eV, as can be seen in Fig. 1.

Kinks. Intriguing kink features in the band dispersion were recently observed: a sharp kink at ∼60 meV, likely of phonon origin, and a broad high-energy kink at ∼0.3 eV below the Fermi level.[22] Since $SrVO_3$ is a Pauli-paramagnetic metal without any signature of magnetic fluctuations, the presence of a kink at high energy suggests a mechanism which is not related to spin fluctuations. Previous calculations based on the LDA + DMFT scheme explained the high-energy kink as purely of electronic origin.[27] We also observe visible broad kinks between −0.1 and −0.4 eV in the vicinity of the Γ point in the GW + DMFT band structure as can be seen in the lower panel of Fig. 1, where one of the GW + DMFT bands is plotted against a renormalized GW band, as was similarly done in Ref. 27. The broad kinks can be recognized as deviations from a parabolic band. The origin of these kinks may be traced back to the deviation from a linear behavior of ReΣ between −0.5 and +0.5 eV as may be seen in Fig. 2.[56] As we scan the straight line $\omega - \varepsilon_{\mathbf{k}n}$ from the Γ point along Γ-R or Γ-X, the crossing with ReΣ, which is the position of the quasiparticle, experiences an oscillation resulting in a kink in the quasiparticle dispersion.

B. Static vs dynamic U

The major effect of the dynamic U is the reduction in the quasiparticle weight or the Z factor, as can be inferred from the slope of the Matsubara-axis self-energy at $\omega = 0$ [$Z \approx 1/(1 - \mathrm{Im}\Sigma(i\omega_0)/\omega_0)$], which is larger in the dynamic than the static U case (Fig. 3). This reduction in the quasiparticle weight is due to the coupling to the high-energy plasmon excitations,

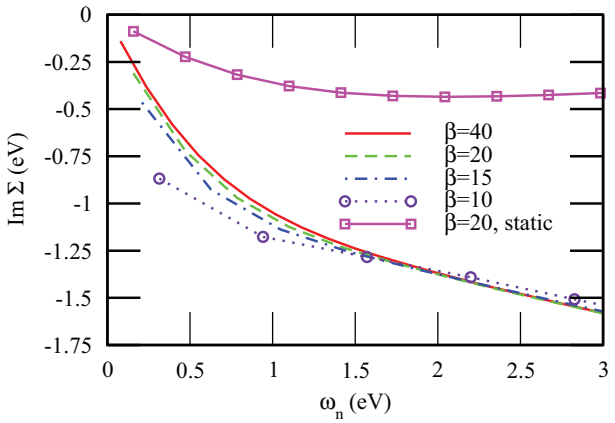

FIG. 3. (Color online) ImΣ as a function of inverse temperature β along the Matsubara axis.

missing in the static U calculation. In Fig. 3 we can also see the dependence of the DMFT self-energy on temperature. Our calculations indicate a possible small deviation from Fermi liquid behavior as the temperature is increased above $T \gtrsim 0.1$, but this should be taken with caution since there are not enough data points close to $\omega = 0$.

The reduction in the Z factor due to the dynamic U results in a band narrowing. This band narrowing has been interpreted in a previous work[57] as the result of a two-step process: first the high-energy part of U renormalizes the one-particle LDA band via the self-energy, and then the remaining low-energy U, which is approximately the static U, renormalizes these bands further, so that the final bandwidth is significantly narrower than the one obtained from just the static U. It was then argued that in order to obtain the same band narrowing as in the full calculation with dynamic U, the starting bandwidth should be reduced if the static cRPA U is to be used.[57] Indeed, to achieve the experimentally observed band narrowing a larger static U (∼5 eV), compared with the static cRPA U of 3.4 eV, is needed in DMFT calculations. The larger static U however leads to an inconsistency: While the band narrowing or the mass enhancement is correct, the separation of the Hubbard bands becomes too large.[26,34] For example, the lower Hubbard band came out too low at ∼−2.5 eV in Refs. 26 and 27. The GW + DMFT total spectral function is shown in Fig. 4 where a broad lower Hubbard band is found centered at −1.5 eV, in agreement with recent photoemission data by Yoshida *et al.*[20] No conclusive data are available for the upper Hubbard band but our theoretical calculation predicts its position at about 2 eV above the Fermi level.

From Fig. 2 it can be inferred that the lower Hubbard band corresponding to the occupied state at the Γ point has higher intensity than the one corresponding to the unoccupied state at the R point.[20] Conversely, the upper Hubbard band corresponding to the unoccupied state at the R point is more prominent than the one corresponding to the occupied state at the Γ point. Moreover, it is also clear that the position of the Hubbard band arising from the state at the Γ point is at approximately 1.5 eV above the Fermi level, lower than the one arising from the state at the R point, which lies at approximately 2.5 eV. Thus, there is a strong dispersion in the upper Hubbard band.

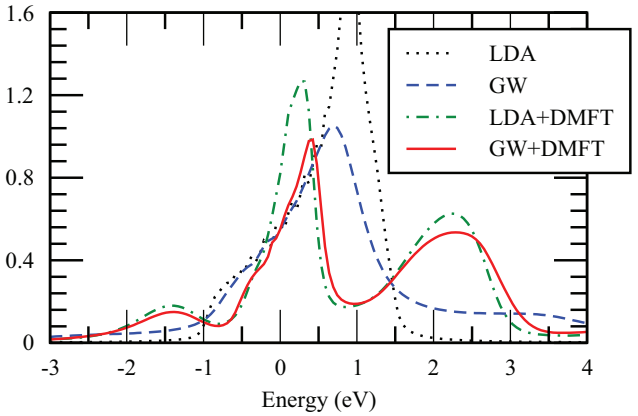

FIG. 4. (Color online) The total spectral function within LDA, GWA, LDA + DMFT, and GW + DMFT.

C. Double-counting correction and vertex correction

In Fig. 5 we compare the DMFT and GW impurity self-energies. The two self-energies are aligned so that the difference in $\mathrm{Re}\Sigma$ is zero at the Fermi level, because the GW self-energy has not been calculated self-consistently. This alignment is crucial to avoid a problem with negative spectral weight and to obtain a physically meaningful spectral function. The difference between the impurity self-energies obtained from the DMFT and the GWA, shown in the right-hand panel of Fig. 5, may be regarded as an onsite vertex correction to the GW self-energy and it is at the heart of the GW + DMFT scheme. It becomes evident that the vertex correction introduces on top of the GW self-energy a strong peak in $\mathrm{Im}\Sigma$ at 1 eV and consequently a strong variation in $\mathrm{Re}\Sigma$ leading to the formation of a satellite at about 2 eV above the Fermi level. On the other hand, we find a weaker peak in $\mathrm{Im}\Sigma$ below the Fermi level and accordingly a broad

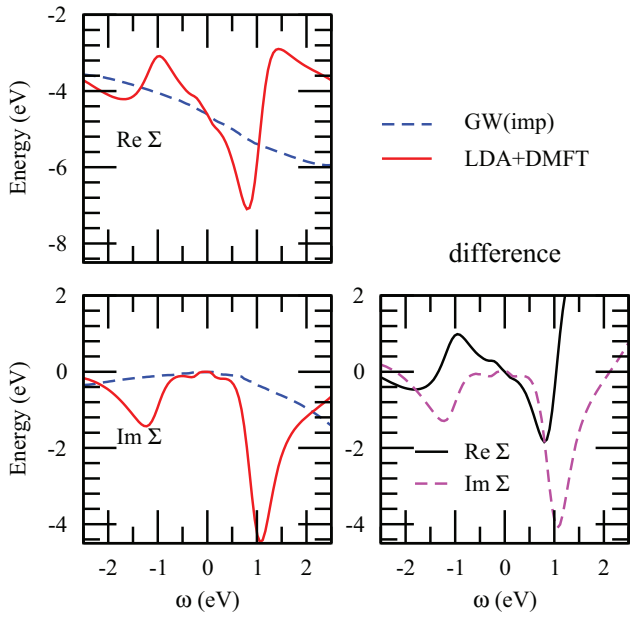

FIG. 5. (Color online) The DMFT and GW impurity self-energies and the vertex correction, which is the difference between the two self-energies.

incoherent structure in the spectral function (see Fig. 4) as found experimentally by Yoshida *et al.*[20]

D. Comparison with previous works

It is appropriate at this point to make a comparison with previous works on $SrVO_3$. The GW + DMFT scheme employed in the work of Tomczak *et al.*[34] goes a step further compared with the scheme used in the present work. In their work, starting from the LDA band structure, a one-shot GW calculation was performed and then a self-consistent DMFT calculation was carried out in which the nonlocal part of this (fixed) GW self-energy was added to the impurity self-energy, whereas in the present scheme we perform two independent calculations, GW and DMFT, and add the two self-energies taking into account double counting. The quasiparticle band structure was not calculated in the work of Tomczak *et al.*,[34] but from the calculated angular-resolved spectra at a few high-symmetry points it is possible to make a partial comparison with the present work. While the lower and upper Hubbard bands are in good agreement with the present work, two prominent discrepancies can be observed. First, the positions of the GW quasiparticle energies at the Γ and X points deduced from the calculated spectra in Fig. 3 of Ref. 34 differ from the result of the present work by a shift of 0.3 eV. Our result agrees very well with a recent quasiparticle calculation of Gatti and Guzzo,[32] and the origin of the discrepancy may be due to the determination of the Fermi level in GWA. Second, the energy difference between the occupied band at the Γ point and the unoccupied band at the X point is essentially unchanged in going from GW to GW + DMFT suggesting that the GW + DMFT quasiparticle band structure is almost the same as the GW one. This is in contrast to the present work where a substantial band reduction is found as shown in Fig. 1. The band reduction is a natural consequence of the vertex correction which enhances the slope of the real part of the GW self-energy leading to a stronger band renormalization, as shown in Fig. 5.

We should also mention two other works related to the present one. Huang and Wang[31] applied the LDA + U scheme with dynamic U on $SrVO_3$ and showed a substantial influence of the frequency dependence of U on the spectral function leading to a larger renormalization of the spectral weight near the Fermi level and an increase in the effective mass as well as a reduction of the t_{2g} band width compared to the conventional LDA + U results with a static U. Another related work is due to Taranto *et al.*[35] in which they compared GW + DMFT and LDA + DMFT schemes using $SrVO_3$ as a test material. The DMFT calculations, however, were performed with a static, rather than a dynamic U. Their main conclusion is that GW + DMFT with a static U obtained from a locally unscreened interaction (or from constrained RPA) and LDA + DMFT with a static U obtained from constrained LDA yield similar self-energies and spectral functions at the Fermi level but the former produces Hubbard bands in better agreement with experiment.

Gatti and Guzzo[32] took a different approach to calculating the spectral function of $SrVO_3$ by employing the cumulant expansion on top of the GWA. The cumulant expansion was originally intended to improve the description of plasmon

satellites in the GWA, which usually overestimates the plasmon binding energy.[58,59] In the GWA, the low-energy satellite above the Fermi level, which may be interpreted as a subplasmon arising from electrons in the narrow t_{2g} band, is also placed too high in energy. Applying the cumulant expansion lowers the satellite binding energy, in good agreement with the result obtained within the GW + DMFT scheme. However, the GWA does not yield any satellite below the Fermi level and no satellite is obtained upon adding the cumulant expansion. The GW quasiparticle band structure essentially remains unchanged with the inclusion of the cumulant so that the bandwidth is still too large compared with experiment.

IV. SIMPLIFIED GW + DMFT SCHEMES

A. GW self-energy at the quasiparticle level

Since GW calculations are computationally expensive, it is fruitful to devise a simplified GW + DMFT scheme that substantially reduces the computational effort but retains the accuracy of the quasiparticle band structure. The idea which we explore first is to maintain the GW self-energy contribution to the quasiparticle energies but to sacrifice its contribution to the spectra, which means that the DMFT self-energy solely determines the spectra. In this way the GW self-energy is only required for a small energy range corresponding to the quasiparticle band width. Apart from reducing the computational effort, this scheme avoids two potential problems that may arise in the original GW + DMFT scheme: First, the imaginary part of the GW self-energy has excitations corresponding to the (Hubbard) satellites at too high energies and these excitations may remain after the removal of the double-counting correction, resulting in spurious satellite peaks at too high energies. Second, there is no guarantee that the GW + DMFT scheme is causal or in other words, the removal of the double-counting correction may result in negative spectral functions. If the DMFT self-energy only determines the spectra, causality is retained.

In the proposed simplified scheme, the interacting Green's function is evaluated as

$$G_{\mathbf{k}n}(\omega) = \frac{1}{\omega - E_{\mathbf{k}n} - [\Sigma^{\mathrm{imp}}(\omega) - \mathrm{Re}\Sigma^{\mathrm{imp}}(E_{\mathbf{k}n})]} \approx \frac{1}{\omega - E^{GW}_{\mathbf{k}n} - \left[\Sigma^{\mathrm{imp}}(\omega) - \mathrm{Re}\Sigma^{\mathrm{DC}}_{nn}\left(E^{GW}_{\mathbf{k}n}\right)\right]}, \quad (6)$$

where $E_{\mathbf{k}n}$ is the quasiparticle energy obtained from Eq. (5) in the full GW + DMFT (as described in Sec. II) scheme and $E^{GW}_{\mathbf{k}n}$ is the GW quasiparticle energy. $\Sigma^{\mathrm{DC}}_{nn}(E_{\mathbf{k}n})$ is the double-counting term given in Eq. (2). In this scheme, the quasiparticle energies are, by construction, the same as in the full scheme but the spectral function is determined by the impurity self-energy. Since the impurity self-energy has the correct analytic properties the spectral function obtained from Eq. (6) does not suffer from the problem of negative spectra, which often arises when two self-energies are subtracted. In Fig. 6 we compare the spectral functions obtained using the full and the simplified scheme. As can be seen, there is little difference between the two spectra indicating that the simplified scheme is comparable in accuracy with the full scheme.

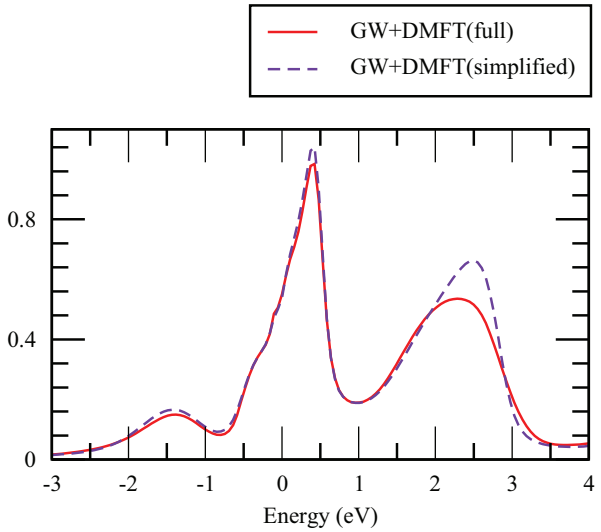

FIG. 6. (Color online) Comparison of the spectral functions calculated with the full GW + DMFT scheme and the simplified scheme [Eq. (6)].

B. DMFT starting from the GW quasiparticle band structure

The second simplified scheme follows the spirit of the original LDA + DMFT scheme, but one starts from the GW band structure instead of the LDA one and performs a DMFT calculation using a static U. It has been observed for a long time that the major effect of the frequency dependence of U which is carried over into the frequency-dependent self-energy on the low-energy spectra is to renormalize the quasiparticle dispersion. Recently, this effect was formally described for a Hubbard-Holstein model Hamiltonian by means of the Lang-Firsov transformation.[57] It is very appealing to apply this idea of quasiparticle renormalization to simplify the GW + DMFT scheme. Starting from the LDA band structure, one first calculates the self-energy within the GW approximation and renormalizes the LDA one-particle dispersion. The resulting renormalized quasiparticle band structure contains the effects of the frequency dependence as well as the momentum dependence of the self-energy. It is then argued that when performing a DMFT calculation starting from the GW quasiparticle band structure, it is only necessary to consider the static U, since the effects of the frequency dependence of U has been included in the starting band structure.

The formal expression for the Green function in the second simplified GW + DMFT scheme is the same as in the second line of Eq. (6):

$$G_{\mathbf{k}n}(\omega) = \frac{1}{\omega - E^{GW}_{\mathbf{k}n} - \left[\tilde{\Sigma}^{\mathrm{imp}}(\omega) - \mathrm{Re}\tilde{\Sigma}^{\mathrm{DC}}_{nn}\left(E^{GW}_{\mathbf{k}n}\right)\right]}, \quad (7)$$

but $\tilde{\Sigma}^{\mathrm{DC}}_{nn}(E_{\mathbf{k}n})$ is the double-counting term given in Eq. (2) with the screened interaction W calculated from a *static* U. Unlike in the LDA + DMFT scheme, the double-counting term is a momentum- and band-dependent quantity. The local self-energy $\tilde{\Sigma}^{\mathrm{imp}}(\omega)$ is obtained by solving the impurity problem within the DMFT scheme with a *static* U. (The tilde denotes that the calculation has been performed with a static U.)

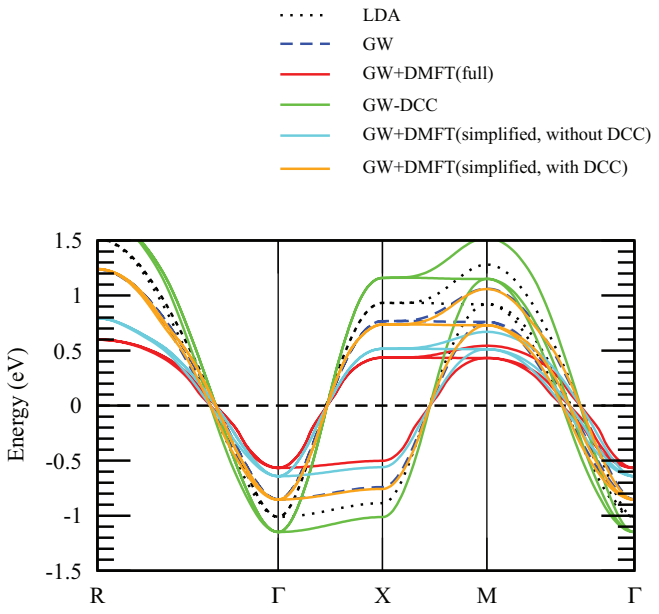

FIG. 7. (Color online) Quasiparticle band structures calculated with the simplified scheme. The label "DCC" denotes the double-counting correction. The results obtained with LDA, GW, and the full $GW+$DMFT are also shown for comparison.

In this second simplified scheme the role of the GW self-energy is to modify the quasiparticle dispersion only but otherwise the frequency-dependent GW self-energy is removed from the Green function. As in the first simplified scheme, this has the advantage of avoiding an inherent problem of the GW approximation in which the positions of satellites are usually overestimated. If the full frequency-dependent GW self-energy is retained there is a possibility that the incorrectly positioned GW satellites remain even after the double-counting term is removed. In the simplified scheme, the satellite structure is entirely determined by the DMFT self-energy, which places the satellites or Hubbard bands at the right energies.

To see how such a scheme works in practice, we show in Fig. 7 the quasiparticle band structures obtained using the second simplified $GW+$DMFT scheme with and without the double-counting correction. There is a close agreement between the quasiparticle band structure *without* the double-counting correction and the quasiparticle band structure obtained with the full scheme. The agreement however deteriorates when the double-counting term is included. A similar calculation has also been presented by Taranto *et al.*[35] in which a DMFT calculation was performed starting from the GW quasiparticle band structure. From the spectral function, one can deduce that the bottom of the t_{2g} band is approximately at -0.5 eV, which is in good agreement with the present calculation *without* the double-counting correction.

It is worth mentioning that the order in which the double-counting correction is introduced is important. The double-counting correction is taken into account *after* performing the self-consistent DMFT loop. When the double-counting term is included *within* the DMFT self-consistent loop, the quasiparticle bandwidth becomes too large. This may be understood from the fact that the starting GW band structure with the double-counting correction included has a bandwidth that is even larger than the LDA one, as can be seen in Fig. 7. The present study suggests that the DMFT calculation should be performed starting from a band structure that is close to the experimental one and the double-counting term should be removed after the DMFT self-consistency loop. This may explain the discrepancy between the present result and that of Tomczak *et al.*[34] In the latter the starting point is the GW self-energy including the double-counting correction, which effectively corresponds to a quasiparticle band structure with a too-wide bandwidth, similar to the one in Fig. 7 (the curve labeled "GW-DCC"). This ambiguity disappears when the $GW+$DMFT scheme is applied fully self-consistently. It would be very interesting to carry out fully self-consistent $GW+$DMFT calculations in which the GW self-energy is also determined self-consistently. Self-consistent GW calculations on molecules have yielded favorable results for ionization potentials[60] and excitation energies.[61] Work on the electron gas on the other hand has shown that fully self-consistent GW calculations yield unsatisfactory spectra.[62] However, the inclusion of vertex corrections by means of the impurity self-energy may change the picture.

V. SUMMARY

In summary, we have performed calculations of the quasiparticle band structure as well as the spectral function of $SrVO_3$ within a simple version of $GW+$DMFT. While the bottom of the occupied GW band is too deep (-0.9 eV) and the result from DMFT with dynamic U too high (-0.4 eV), the $GW+$DMFT scheme yields a value of -0.6 eV, which is in good agreement with the experimental value of -0.7 eV. From the point of view of the GWA the result illustrates the importance of onsite vertex corrections whereas from the DMFT point of view it demonstrates the significance of the nonlocal self-energy. The $GW+$DMFT scheme is sufficiently sensitive to yield kink structures in the quasiparticle dispersion between -0.1 and -0.4 eV in the vicinity of the Γ point. A well-defined upper Hubbard band centered at around 2 eV is obtained whereas a rather broad incoherent feature is found below the quasiparticle peak centered at around -1.5 eV. Our calculations also indicate a possible deviation from Fermi liquid behavior as the temperature is increased above $T \gtrsim 0.1$.

We have also considered two simplified schemes, in which the contribution of the GW self-energy is restricted to the quasiparticle band. In the first scheme the quasiparticle band structure is by construction identical to that of the full scheme and the spectral functions are found to be in very close agreement with those of the full scheme. This scheme is computationally advantageous because it avoids the calculation of the GW self-energy over a wide energy range. In the second scheme, the GW quasiparticle band structure is used as a starting point for DMFT calculations with a static U. It is found that the resulting bandwidth is too large compared with the result of the full scheme.

ACKNOWLEDGMENTS

We would like to thank S. Biermann for reading the manuscript and for many useful comments. We would also like to thank C. Friedrich and S. Blügel for providing us with

their FLAPW code, and M. Casula and T. Miyake for fruitful discussions. This work was supported by the Swedish Research Council and "Materials Design through Computics: Complex Correlation and Non-Equilibrium Dynamics," a Grant in Aid for Scientific Research on Innovative Areas, MEXT, Japan, and by the Scandinavia-Japan Sasakawa Foundation. P.W. acknowledges support from SNF Grant No. 200021_140648. The computations were performed on resources provided by the Swedish National Infrastructure for Computing (SNIC) at LUNARC, and on the Brutus cluster at ETH Zurich.

[1] W. Metzner and D. Vollhardt, Phys. Rev. Lett. **62**, 324 (1989).
[2] A. Georges and G. Kotliar, Phys. Rev. B **45**, 6479 (1992).
[3] A. Georges, G. Kotliar, W. Krauth, and M. J. Rozenberg, Rev. Mod. Phys. **68**, 13 (1996).
[4] V. I. Anisimov, A. I. Poteryaev, M. A. Korotin, A. O. Anokhin, and G. Kotliar, J. Phys.: Condens. Matter **9**, 7359 (1997).
[5] A. I. Lichtenstein and M. I. Katsnelson, Phys. Rev. B **57**, 6884 (1998).
[6] G. Kotliar, S. Y. Savrasov, K. Haule, V. S. Oudovenko, O. Parcollet, and C. A. Marianetti, Rev. Mod. Phys. **78**, 865 (2006).
[7] K. Held, Adv. Phys. **56**, 829 (2007).
[8] L. Hedin, Phys. Rev. **139**, A796 (1965).
[9] F. Aryasetiawan and O. Gunnarsson, Rep. Prog. Phys. **61**, 237 (1998).
[10] W. G. Aulbur, L. Jönsson, and J. W. Wilkins, Solid State Phys. **54**, 1 (1999).
[11] G. Onida, L. Reining, and A. Rubio, Rev. Mod. Phys. **74**, 601 (2002).
[12] T. Miyake, C. Martins, R. Sakuma, and F. Aryasetiawan, Phys. Rev. B **87**, 115110 (2013).
[13] S. Biermann, F. Aryasetiawan, and A. Georges, Phys. Rev. Lett. **90**, 086402 (2003).
[14] K. Morikawa, T. Mizokawa, K. Kobayashi, A. Fujimori, H. Eisaki, S. Uchida, F. Iga, and Y. Nishihara, Phys. Rev. B **52**, 13711 (1995).
[15] I. H. Inoue, O. Goto, H. Makino, N. E. Hussey, and M. Ishikawa, Phys. Rev. B **58**, 4372 (1998).
[16] A. Sekiyama, H. Fujiwara, S. Imada, S. Suga, H. Eisaki, S. I. Uchida, K. Takegahara, H. Harima, Y. Saitoh, I. A. Nekrasov, G. Keller, D. E. Kondakov, A. V. Kozhevnikov, Th. Pruschke, K. Held, D. Vollhardt, and V. I. Anisimov, Phys. Rev. Lett. **93**, 156402 (2004).
[17] T. Yoshida, K. Tanaka, H. Yagi, A. Ino, H. Eisaki, A. Fujimori, and Z.-X. Shen, Phys. Rev. Lett. **95**, 146404 (2005).
[18] R. Eguchi, T. Kiss, S. Tsuda *et al.*, Phys. Rev. Lett. **96**, 076402 (2006).
[19] M. Takizawa, M. Minohara, H. Kumigashira, D. Toyota, M. Oshima, H. Wadati, T. Yoshida, A. Fujimori, M. Lippmaa, M. Kawasaki, H. Koinuma, G. Sordi, and M. Rozenberg, Phys. Rev. B **80**, 235104 (2009).
[20] T. Yoshida, M. Hashimoto, T. Takizawa, A. Fujimori, M. Kubota, K. Ono, and H. Eisaki, Phys. Rev. B **82**, 085119 (2010).
[21] K. Yoshimatsu, K. Horiba, H. Kumigashira, T. Yoshida, A. Fujimori, and M. Oshima, Science **333**, 319 (2011).
[22] S. Aizaki, T. Yoshida, K. Yoshimatsu, M. Takizawa, M. Minohara, S. Ideta, A. Fujimori, K. Gupta, P. Mahadevan, K. Horiba, H. Kumigashira, and M. Oshima, Phys. Rev. Lett. **109**, 056401 (2012).
[23] K. Maiti, D. D. Sarma, M. J. Rozenberg, I. H. Inoue, H. Makino, O. Goto, M. Pedio, and R. Cimino, Europhys. Lett. **55**, 246 (2001).
[24] A. Liebsch, Phys. Rev. Lett. **90**, 096401 (2003).
[25] E. Pavarini, S. Biermann, A. Poteryaev, A. I. Lichtenstein, A. Georges, and O. K. Andersen, Phys. Rev. Lett. **92**, 176403 (2004).
[26] K. Maiti, U. Manju, S. Ray, P. Mahadevan, I. H. Inoue, C. Carbone, and D. D. Sarma, Phys. Rev. B **73**, 052508 (2006).
[27] I. A. Nekrasov, K. Held, G. Keller, D. E. Kondakov, Th. Pruschke, M. Kollar, O. K. Andersen, V. I. Anisimov, and D. Vollhardt, Phys. Rev. B **73**, 155112 (2006).
[28] M. Karolak, T. O. Wehling, F. Lechermann, and A. I. Lichtenstein, J. Phys.: Condens. Matter **23**, 085601 (2011).
[29] M. Casula, A. Rubtsov, and S. Biermann, Phys. Rev. B **85**, 035115 (2012).
[30] H. Lee, K. Foyevtsova, J. Ferber, M. Aichhorn, H. O. Jeschke, and R. Valenti, Phys. Rev. B **85**, 165103 (2012).
[31] L. Huang and Y. Wang, Europhys. Lett. **99**, 67003 (2012).
[32] M. Gatti and M. Guzzo, Phys. Rev. B **87**, 155147 (2013).
[33] R. Sakuma, T. Miyake, and F. Aryasetiawan, Phys. Rev. B **86**, 245126 (2012).
[34] J. M. Tomczak, M. Casula, T. Miyake, F. Aryasetiawan, and S. Biermann, Europhys. Lett. **100**, 67001 (2012).
[35] C. Taranto, M. Kaltak, N. Parragh, G. Sangiovanni, G. Kresse, A. Toschi, and K. Held, Phys. Rev. B **88**, 165119 (2013).
[36] P. Sun and G. Kotliar, Phys. Rev. Lett. **92**, 196402 (2004).
[37] T. Ayral, P. Werner, and S. Biermann, Phys. Rev. Lett. **109**, 226401 (2012).
[38] T. Ayral, S. Biermann, and P. Werner, Phys. Rev. B **87**, 125149 (2013).
[39] P. Hansmann, T. Ayral, L. Vaugier, P. Werner, and S. Biermann, Phys. Rev. Lett. **110**, 166401 (2013).
[40] A. N. Rubtsov, V. V. Savkin, and A. I. Lichtenstein, Phys. Rev. B **72**, 035122 (2005).
[41] P. Werner, A. Comanac, L. de Medici, M. Troyer, and A. J. Millis, Phys. Rev. Lett. **97**, 076405 (2006).
[42] P. Werner and A. J. Millis, Phys. Rev. B **74**, 155107 (2006).
[43] P. Werner and A. J. Millis, Phys. Rev. Lett. **99**, 146404 (2007).
[44] F. F. Assaad and T. C. Lang, Phys. Rev. B **76**, 035116 (2007).
[45] P. Werner and A. J. Millis, Phys. Rev. Lett. **104**, 146401 (2010).
[46] P. Werner, M. Casula, T. Miyake, F. Aryasetiawan, A. J. Millis, and S. Biermann, Nat. Phys. **8**, 331 (2012).
[47] N. Marzari and D. Vanderbilt, Phys. Rev. B **56**, 12847 (1997).
[48] I. Souza, N. Marzari, and D. Vanderbilt, Phys. Rev. B **65**, 035109 (2001).
[49] R. Sakuma, Phys. Rev. B **87**, 235109 (2013).
[50] A. A. Mostofi, J. R. Yates, Y.-S. Lee, I. Souza, D. Vanderbilt, and N. Marzari, Comput. Phys. Commun. **178**, 685 (2008).
[51] F. Aryasetiawan, M. Imada, A. Georges, G. Kotliar, S. Biermann, and A. I. Lichtenstein, Phys. Rev. B **70**, 195104 (2004).
[52] L. Hedin, J. Phys.: Condens. Matter **11**, R489 (1999).
[53] http://www.flapw.de/.
[54] C. Friedrich, S. Blügel, and A. Schindlmayr, Phys. Rev. B **81**, 125102 (2010).

[55]A fully self-consistent GW + DMFT treatment, beyond the scope of this work, may lead to modifications in the balance between local and nonlocal correlations.[38]

[56]The real-frequency impurity self-energy has been obtained by maximum entropy analytical continuation of the auxiliary Green's function $G^{\rm imp}_{\rm aux} = 1/(i\omega_n + \mu_{\rm aux} - \Sigma^{\rm imp}(i\omega_n))$, where $\mu_{\rm aux}$ was chosen by minimizing the difference between the back-transformed Matsubara-axis self-energy and the original CT-QMC data.

[57]M. Casula, Ph. Werner, L. Vaugier, F. Aryasetiawan, T. Miyake, and A. J. Millis, and S. Biermann, Phys. Rev. Lett. **109**, 126408 (2012).

[58]F. Aryasetiawan, L. Hedin, and K. Karlsson, Phys. Rev. Lett. **77**, 2268 (1996).

[59]M. Guzzo, G. Lani, F. Sottile, P. Romaniello, M. Gatti, J. J. Kas, J. J. Rehr, M. G. Silly, F. Sirotti, and L. Reining, Phys. Rev. Lett. **107**, 166401 (2011).

[60]C. Rostgaard, K. W. Jacobsen, and K. S. Thygesen, Phys. Rev. B **81**, 085103 (2010).

[61]F. Caruso, P. Rinke, X. Ren, M. Scheffler, and A. Rubio, Phys. Rev. B **86**, 081102(R) (2012).

[62]B. Holm and U. von Barth, Phys. Rev. B **57**, 2108 (1998).